The promotional effect of rare-earth on Pt for ethanol electrooxidation and its application on DEFC

Alécio Rodrigues Nunes [1], José J. Linares [2], Rudy Crisafulli [2], Sabrina C. Zignani [3], and Flávio Colmati [1,*]

[1] Instituto de Química, Universidade Federal de Goiás, Avenida Esperança s/n, Campus Samambaia, 74690-900 Goiânia (Goiás) Brazil
[2] Institute of Chemistry, University of Brasilia, Campus Universitário Darcy Ribeiro, 70910-900 Brasilia, Brazil
[3] ITAE—Istituto di Tecnologie Avanzate per l'Energia "Nicola Giordano", National Research Council of Italy, Salita Santa Lucia Sopra Contesse, 5, 98126 Messina, Italy
*Correspondence: colmati@ufg.br

Figure S1 shows the catalysts' blank cyclic voltammograms (CV) in acid and alkaline mediums. As can be observed, the format of the voltammograms is similar regardless of the presence of the auxiliary rare-earth metals. The PtC signal is larger than the bimetallic materials due to the higher loading (given that the amount of deposited material is the same for the four electrodes). Peaks attributed to the hydrogen adsorption/desorption regions appear in all the materials for the acid and alkaline blanks, as well as the Pt oxide formation/reduction peaks at higher potentials. In this way, the presence of the auxiliary rare-earth metals does not alter the typical peaks of polycrystalline platinum.
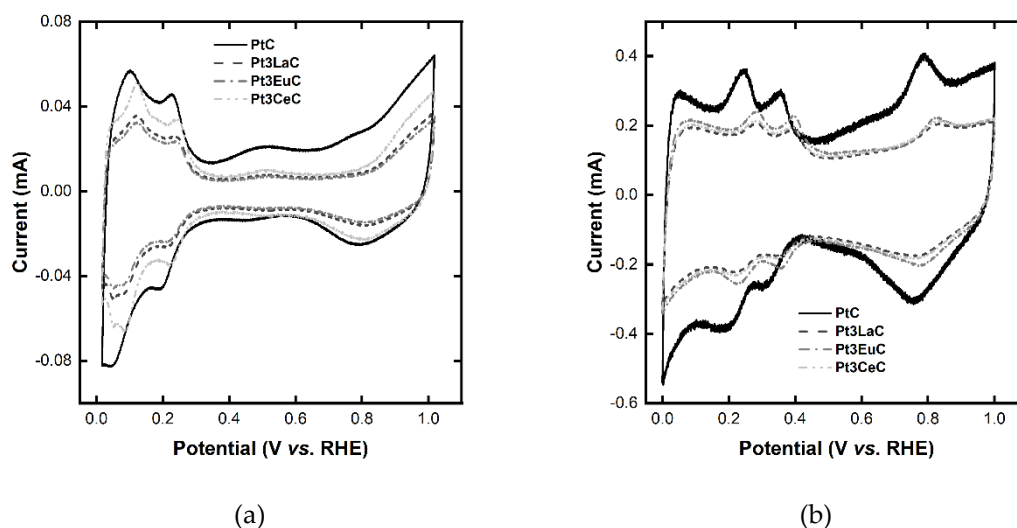

(a)   (b)

Figure S1. Blank CV of the electrocatalysts in (a) 0.5 mol L^{-1} H_2SO_4 and (b) 1 mol L^{-1} KOH

Figure S2 displays the CO stripping profiles of the different catalysts. Table S1 collects the corresponding onset potentials for the CO electrooxidation reaction and the electrochemically active surface area (EASA) values from this measurement. Equation S1 allows estimating the EASA (m^2 g^{-1}), where A (mA $\cdot$V) is the area difference between the CO stripping peaks (1st cycle) and the baseline (3rd cycle), υ is the scan rate (V s^{-1}), m is the mass of Pt (g) and 4200 mC m^{-2} is the surface charge associated with the oxidation of CO [1].

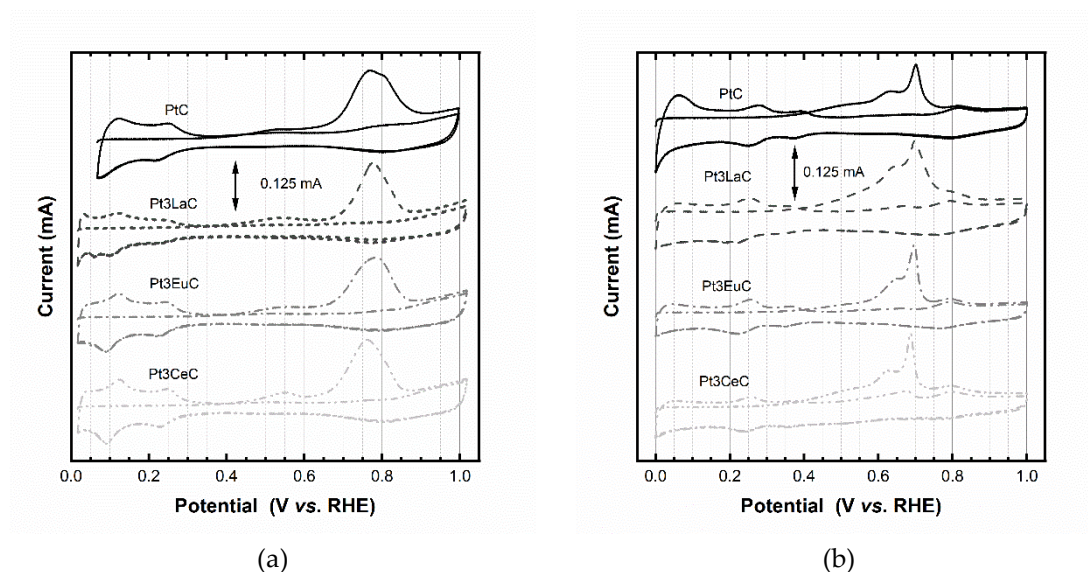$$EASA = \frac{A}{\upsilon \cdot m \cdot 4200} \qquad (S1)$$

Figure S2. Blank CV of the electrocatalysts in (a) 0.5 mol L^{-1} H_2SO_4 and (b) 1 mol L^{-1} KOH

Table S1. Onset potential and EASA extracted from the CO stripping experiments.

Catalyst	Acid medium		Alkaline medium	
	Onset potential (mV)	EASA (m^2 g^{-1} Pt)	Onset potential (mV)	EASA (m^2 g^{-1} Pt)
PtC	448	15.1	407	19.8
Pt3LaC	356	16.4	388	27.3
Pt3EuC	393	17.4	399	22.6
Pt3CeC	397	17.6	387	24.1

Adding the rare earth to the catalyst composition leads to a drop in the onset potential for CO oxidation. Their presence impacts the electronic properties of Pt, in addition to oxygenated species coming from the surface of rare earth oxides, resulting in a decreased onset potential. The values of the EASA are used to normalize the currents obtained in the ethanol electrooxidation measurements.

Figure S3 displays the chronoamperometric curves recorded at 0.726 V vs. RHE (see Materials and Methods section of the manuscript for more details). The results confirm the excellent predisposition of the bimetallic materials, which outperform PtC. In particular, Pt3CeC emerges as the best material from its highest performance and less steep decay rate than the other materials. This is due to the synergy between the electronic and bifunctional mechanisms, which alleviates the deactivation of the catalyst surface by the ethanolic residues formed during the EEO reaction.

Figure S4 shows the power density curves of the different materials. Confirming the polarization curves, adding rare earth metals to the catalyst formulation, especially in the case of Pt3CeC, is notoriously beneficial for increasing the power density. If we compare these results with those obtained for the active Pd-based in alkaline medium, presented in a recent review by Souza et al. [2] and Pinheiro et al. [3], our results present lower maximum power densities than Pd/C and the bimetallic materials (with Ru, Sn, Ni, Nb, Ir and $NaNbO_3$, in the range of 15 to 176 mW cm^{-2}). The same conclusion can be drawn for the operation in acidic medium, when compared to the performance of PtRu/C and PtSn/C (power densities above 50 mW cm^{-2} [4]). Although our results are lower than others reported in the literature, we believe there is still room for improvement based on the non-optimized electrode preparation method.
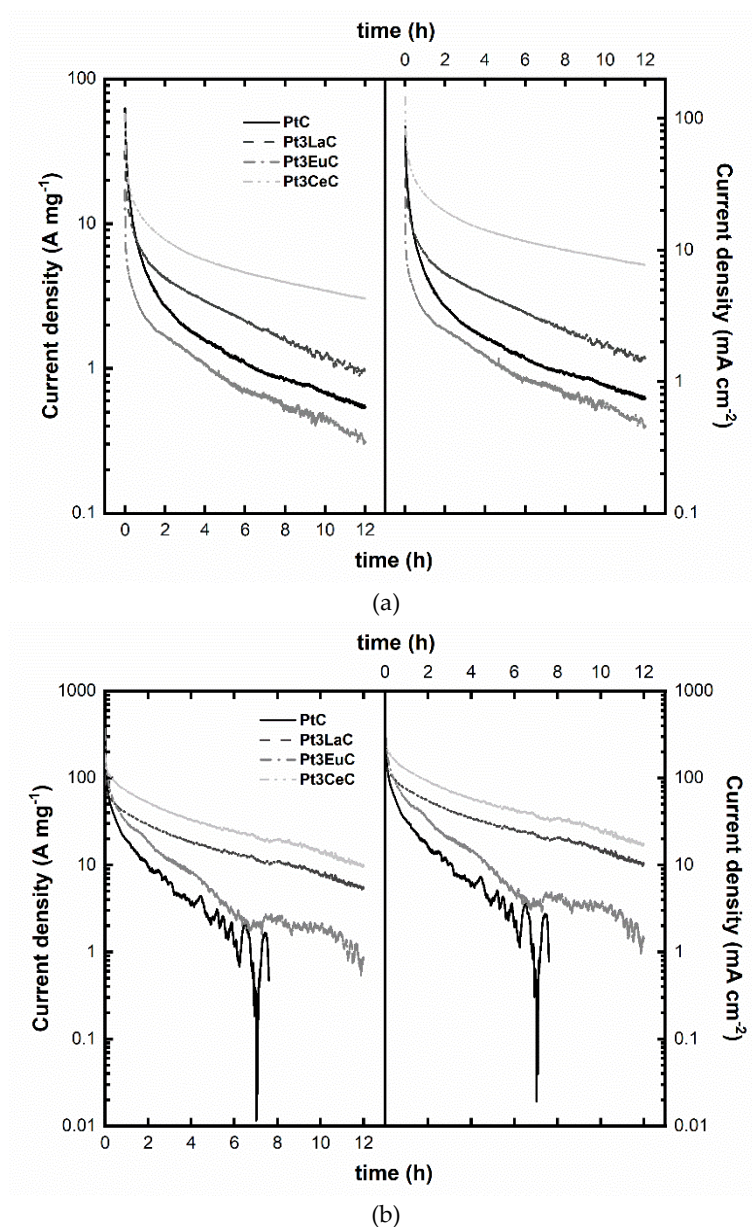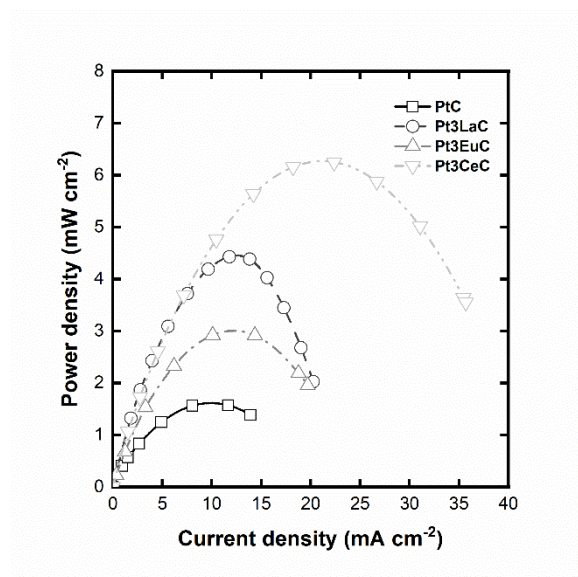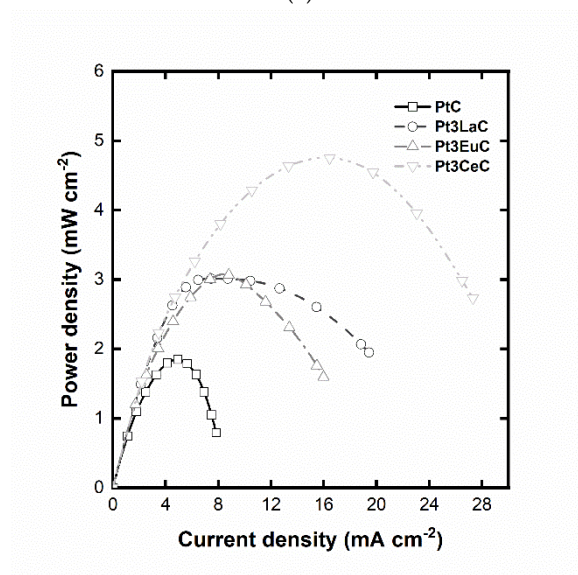
Figure S3. Ethanol electrooxidation curves for the different electrocatalysts in 1 mol L^{-1} ethanol and (a) 0.5 mol L^{-1} H2SO4, and (b) 1 mol L^{-1} KOH (curves are normalized to the mass of Pt and the Pt EASA)

(a)

(b)

Figure S4. Power density curves of the DEFC with different anode fuels (a) 2 mol L^{-1} ethanol, and (b) 2 mol L^{-1} ethanol and 4 mol L^{-1} KOH.

References

1. Binninger, T.; Fabbri, E.; Kötz, R.; Schmidt, T.J. Determination of the Electrochemically Active Surface Area of Metal-Oxide Supported Platinum Catalyst. *J. Electrochem. Soc.* **2014**, *161*, H121–H128, doi:10.1149/2.055403jes.

2. Souza, F.M.; Pinheiro, V.S.; Gentil, T.C.; Lucchetti, L.E.B.; Silva, J.C.M.; L.M.G. Santos, M.; De Oliveira, I.; Dourado, W.M.C.; Amaral-Labat, G.; Okamoto, S.; et al. Alkaline Direct Liquid Fuel Cells: Advances, Challenges and Perspectives. *J. Electroanal. Chem.* **2022**, *922*, 116712, doi:10.1016/j.jelechem.2022.116712.

3. Pinheiro, V.S.; Souza, F.M.; Gentil, T.C.; Nascimento, A.N.; Parreira, L.S.; Hammer, P.; Sairre, M.I.; Batista, B.L.; Santos, M.C. Electrocatalysts Based on Low Amounts of Palladium Combined with Tin Nanoparticles and Cerium Dioxide Nanorods for Application as ADEFC Anodes. *Int. J. Hydrogen Energy* **2021**, *46*, 39438–39456, doi:10.1016/j.ijhydene.2021.09.176.

4. Mukherjee, A.; Basu, S. Direct Hydrocarbon Low-Temperature Fuel Cell. In *Electrocatalysts for Low Temperature Fuel Cells*; Maiyalagan, T., Saji, V.S., Eds.; Wiley-VCH Verlag GmbH & Co. KGaA: Weinheim, Germany, 2017; pp. 113–143.